Journal of Structural Geology 31 (2009) 1365–1376

Contents lists available at ScienceDirect

Journal of Structural Geology

journal homepage: www.elsevier.com/locate/jsg

Strain analysis and rheology contrasts in polymictic conglomerates: An example from the Seine metaconglomerates, Superior Province, Canada

Dyanna M. Czeck [a,*], Darlene A. Fissler [a], Eric Horsman [b], Basil Tikoff [b]

[a] Department of Geosciences, University of Wisconsin-Milwaukee, 3209 N. Maryland Ave., Milwaukee, WI 53211, USA
[b] Department of Geology & Geophysics, University of Wisconsin-Madison, 1215 W Dayton St., Madison, WI 53706, USA

ARTICLE INFO

Article history:
Received 1 October 2008
Received in revised form
10 July 2009
Accepted 3 August 2009
Available online 12 August 2009

Keywords:
Strain analysis
Conglomerate
Effective viscosity
Rheology

ABSTRACT

Deformed conglomerates typically display contrasting strains between different lithological clast populations and matrix, which can be exploited to provide information about effective viscosity contrasts. We analyzed three different clast populations (granitoid, mafic volcanic, and felsic volcanic) across a strain gradient in the Seine metaconglomerates of Ontario, Canada. We calculated finite strain using the R_f/φ method and bootstrap statistics. Granitoid clasts exhibited the least amount of strain, while the mafic and felsic clasts had similar, greater strains. We assumed that the bulk finite strain was recorded by the mafic clasts, given their large proportion of the rock and their similar composition to the matrix. We calculated effective viscosity contrasts using the finite strain information, assuming Newtonian viscous rheology. The two volcanic clast populations have similar effective viscosities, regardless of strain magnitude, with ratios of felsic/mafic ranging from 0.27 to 2.12 and average ratio of 1.19. The granitoid clasts are significantly more competent than the mafic clasts with effective viscosity ratios ranging from 2.35 to 12.39 and average ratio of 5.61. The results are consistent with a qualitative competence hierarchy of granitoid > felsic ≥ mafic, although the quantitative effective viscosity ratios change with strain magnitude. Consequently, the effective viscosity contrast between clast types is strain dependent and possibly deformation path dependent.

1. Introduction

A goal of many structural geology studies is to constrain the rheology of deformation that occurs on geological spatial and temporal scales. All aspects of rock deformation and evolution of tectonic plates are a function of the deformation behavior of rocks over geological time scales. While experimental deformation has been the dominant approach for quantifying rheology (e.g., Kirby, 1985; Kirby and Kronenberg, 1987; Paterson and Luan, 1990; Kohlstedt et al., 1995), it has two major limitations when addressing crustal geological material (e.g., Paterson, 2001). First, experiments occur at strain rates many orders of magnitude faster than geological conditions by heating samples to unnaturally high temperatures, and commonly proceed to only modest total strain. Second, samples typically have small volume and are mineralogically simple. Together, these characteristics call into question the utility of experimental results extrapolated to geological conditions.

Another approach to study rheology is to use field-based information. Although structural geologists are interested in extracting rheological information from rocks (Hudleston and Lan, 1995; Masuda et al., 1995; Talbot, 1999), quantitative information can only be extracted in very particular settings. Approaches that provide rheological information include: 1) wavelength/thickness ratios of ductile instabilities, such as folds and boudinage (Smith, 1975, 1977); 2) fold shapes (Hudleston and Holst, 1984; Hudleston and Lan, 1993); 3) shapes of boudins and mullions (Ramsay, 1967; Hudleston and Lan, 1995); 4) cleavage refraction across deformed layers (Treagus, 1983, 1999); and 5) differences in strain between deformed conglomerate clasts of different lithologies (Lisle et al., 1983; Treagus and Treagus, 2002). Using some of these field approaches, Ramsay (1982) determined a qualitative hierarchy of relative rock competence; however, quantitative assessments are still lacking.

We outline a method using field data from deformed polymictic conglomerates to quantify the relationships between progressive finite strain of various clast types, and thereby constrain the rheology of naturally deformed rocks. We quantify finite strain along a strain gradient in the Seine metaconglomerates, Ontario, Canada. The finite strain data allow us to calculate effective

* Corresponding author. Tel.: +1 414 229 3948.
E-mail address: dyanna@uwm.edu (D.M. Czeck).

0191-8141/$ – see front matter © 2009 Elsevier Ltd. All rights reserved.
doi:10.1016/j.jsg.2009.08.004

viscosity (Treagus and Treagus, 2002). Our results indicate that granitoid clasts typically have a greater effective viscosity than felsic clasts, which have a slightly greater effective viscosity than mafic clasts. The strain gradient between outcrops allows us to determine that relative rock competence is not constant, but depends on strain magnitude and/or strain history.

2. Geologic setting

2.1. Superior Province and Rainy Lake region

The rocks used for this study are the deformed polymictic Seine metaconglomerates located in the Superior Province near the border of Ontario, Canada and Minnesota, USA. The Superior Province (Fig. 1) is part of the stable Archean craton of North America and is comprised of subprovinces that are distinguished based on lithologic differences, metamorphic grade, and structural patterns (Card and Ciesielski, 1986). The central portion of the Superior Province contains alternating metasedimentary and metavolcanic/plutonic subprovinces that are often fault-bounded, or at least unconformable. The assemblage of subprovinces most likely represents repeated collisions of small allochthonous terranes during the Late Archean (e.g., Burke et al., 1976; Langford and Morin, 1976; Hoffman, 1989, 1990; Percival and Williams, 1989; Card, 1990). The volcanic/plutonic subprovinces likely formed from volcanic arcs, and the metasedimentary provinces are likely the metamorphosed equivalent of the basin sediments that accumulated between successive arcs. This area of the Superior Province assembled in the Archean and was largely unaffected by any subsequent tectonic events.

The rocks and structures within the Rainy Lake region of northern Minnesota, USA and adjacent Ontario, Canada straddle the boundary between the Quetico and Wabigoon subprovinces (Figs. 1 and 2). The lithologic and structural assemblage presumably formed during this active tectonic scenario with volcanic arc formation followed by oblique collision of the subprovinces/terranes approximately 2.7 Ga (e.g., Davis et al., 1989). The Quetico subprovince includes mostly metasedimentary rocks of

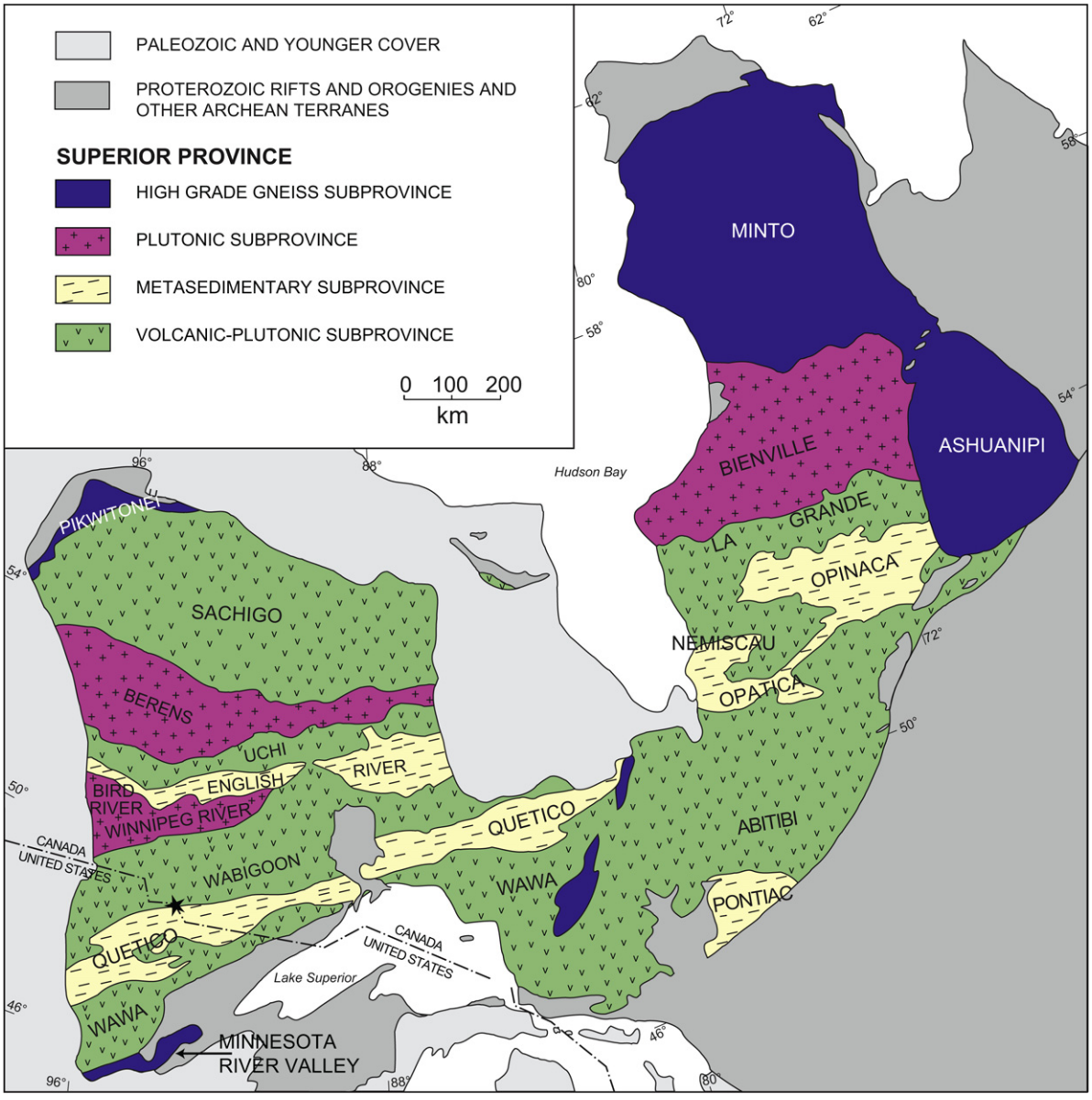

Fig. 1. Simplified geologic map of the Superior Province, modified after Card and Ciesielski (1986) and Marquis (2004). The field area is indicated by a star.

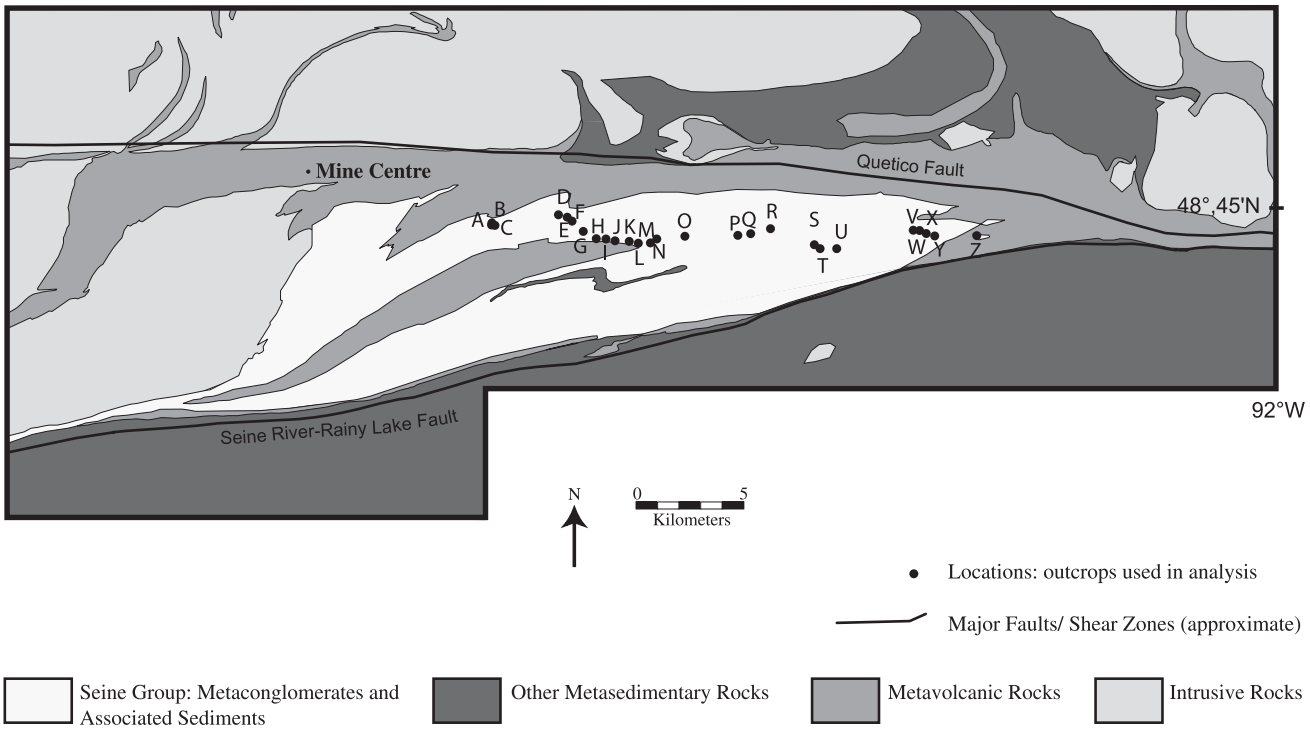

Fig. 2. Simplified geologic map of the region containing the Seine metaconglomerates with strain analysis stations indicated. Modified from Czeck and Hudleston (2003) after Stone et al. (1997a,b) and Wood et al. (1980a,b).

amphibolite grade, and the Wabigoon subprovince mostly consists of older metavolcanic and metaplutonic rocks of greenschist grade (Poulsen, 2000).

The Rainy Lake region is a fault/shear zone-bounded triangular wedge between the Quetico and Wabigoon subprovinces (Fig. 2). The Quetico Fault to the north and the Rainy Lake–Seine River Fault to the south bound this wedge, and these two faults merge to the east and continue for over 200 km (Poulsen, 1986). These structures are typically called faults because they bound stratigraphically discordant units; however, they are shear zones in the respect that they have a ductile fabric within them (Czeck and Fralick, 2002). Ductile shear zones localize strain into an anastomosing network pattern along and between these faults (Poulsen, 1986; Tabor and Hudleston, 1991). The locations of these smaller structures have been determined by the discordant boundaries of the lithostratigraphic terranes and linear features observed on electromagnetic anomaly maps, but cannot typically be directly observed (Poulsen, 1986, 2000). The Seine Group includes the polymictic Seine metaconglomerates (Fig. 3). Based on stratigraphic evidence (Poulsen et al., 1980) and high precision U–Pb dating (Davis et al., 1989; Fralick and Davis, 1999), the Seine Group formed between circa 2692 Ma, the approximate timing for the onset of major deformation, and circa 2686 Ma, the emplacement of the late syntectonic Algoman plutons (Czeck et al., 2006; Druguet et al., 2008). Seine-type sedimentary packages occur in association with strike-slip zones throughout the Superior Province, leading to the conclusion that they may have formed within strike-slip related basins during deformation (Poulsen, 1986).

Peak metamorphic conditions ranged from 400 to 600 °C with pressures of approximately 3 kb (Poulsen, 2000). In general, within the fault-bounded wedge of the Seine River–Rainy Lake and Quetico Faults, the rocks are greenschist facies to the east and amphibolite facies to the west of the main study area (Poulsen, 2000). The Seine Group lies entirely within the greenschist facies.

2.2. Seine Group

The Seine Group consists of interbedded metamorphosed conglomerates and sandstones. The large-scale stratigraphic feature of the unit is a gradual fining-upward transition with a conglomerate-dominated facies at the base and a sandstone-dominated facies at the top (Frantes, 1987; Czeck and Fralick, 2002). Parallel laminations and low angle cross-stratification are common within the sandstone beds (Poulsen, 2000).

The objects of our study are the metaconglomerates within the Seine Group. The best exposures of the metaconglomerates are located along a continuous 23 km stretch of Ontario's Highway 11. The deformed conglomerates are typically clast-supported (with approximately 5 to 30% matrix by volume) and polymictic, containing pebble to boulder-sized metamorphosed clasts of granitoid, felsic volcanic, mafic volcanic, volcanic porphyry, banded iron formation, gabbro, and quartzite lithologies. All clasts within the metaconglomerate are metamorphosed; however, for simplicity, we omit the prefix "meta" when describing rock types. Often within conglomerate exposures, bedding can be identified by channels of metamorphosed sandstones. Qualitatively, strain varies throughout the region and between clast types (Fig. 3). Localized areas of greater strain occasionally have crenulations and small-scale (wavelength typically less than 1 m but up to ~10 m) folds.

We investigated the strain of the three most abundant clast types: granitoid, felsic volcanic, and intermediate to mafic volcanic. Typically, all other clast types volumetrically comprise less than 1% of the rock. Mafic clasts are typically somewhat more abundant than felsic clasts, ranging from 29 to 61% compared to 22 to 48% of clasts at a particular outcrop. Granitoid clasts range from 12 to 38% of clasts at analyzed outcrops.

The matrix has an intermediate-mafic volcanic composition and consists of fine-grained (<0.05 to 0.1 mm) plagioclase feldspar, quartz, hornblende, and chlorite. In more strained samples, grain sizes can be up to approximately 0.3 mm. A strong fabric occurs

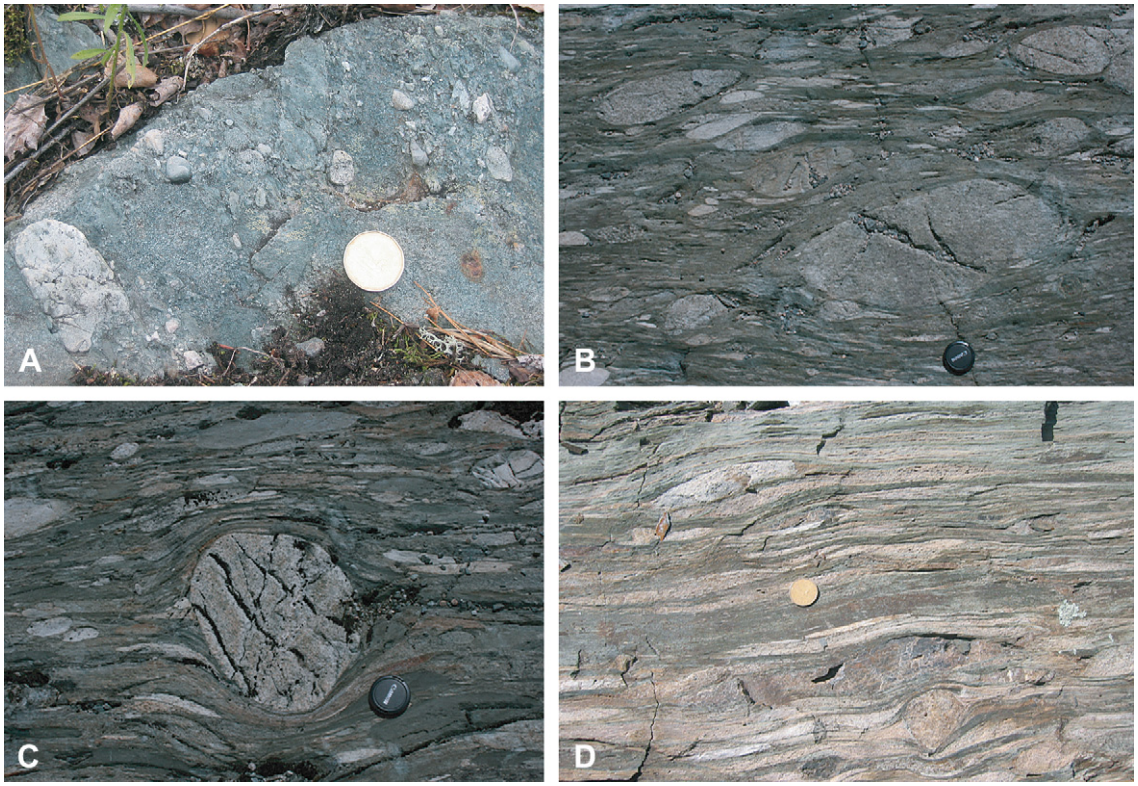

Fig. 3. Examples of weakly (A), moderately (B, C), and strongly (D) strained Seine metaconglomerates. All photos are taken on a subhorizontal surface. For photos A and D, diameter of Canadian $1 coin is 26.5 mm. For photos B and C, diameter of lens cap is 58 mm.

within the matrix at intensely strained outcrops, mostly formed by seams of insoluble material, but also by the preferred alignment of larger grains, especially chlorite and biotite.

Felsic volcanic clasts are composed predominantly of fine-grained quartz, plagioclase, and orthoclase feldspar. Mafic volcanic clasts are composed primarily of fine-grained plagioclase feldspar, quartz, hornblende, and chlorite. Grain sizes are less than approximately 0.05 to 0.1 mm in weakly strained samples, ranging up to 0.3 mm in the strongly strained samples. Occasional orthoclase phenocrysts in the felsic clasts range in size from 0.4 to 0.9 mm. Volcanic clasts have a strong fabric within intensely strained outcrops. In the felsic clasts, stretched quartz is the dominant mineral defining the fabric, whereas chlorite and hornblende are strongly aligned in the mafic clasts. Seams of insoluble material are also present.

Granitoid clasts are typically tonalite, trondhjemite, diorite, or granodiorite in composition. They are predominantly composed of coarse-grained quartz (0.5 to 0.9 mm), plagioclase, and orthoclase feldspar (1–3 mm) with trace amounts of biotite and opaque minerals (0.3 to 0.5 mm, ranging up to 1.2 mm). Foliation within the granitoid clasts is nonexistent to weak, but is formed by alignment of quartz, plagioclase, and, in some cases, biotite when present. Large quartz grains display undulose extinction within the granitoid clasts. In more intensely strained outcrops, some plagioclase grains have lenticular lamellae that bend or kink as they cross earlier twin lamellae. Within some of these strongly strained granitoid clasts, favorably oriented plagioclase grains also display undulose extinction.

2.3. Structural framework

The main structures found at the Wabigoon–Quetico boundary include folds and shear zones. In general, early folds and thrust faults were followed by nearly vertical shear zones and a ubiquitous overprinting, subvertical flattening fabric that formed in dextral transpression (Poulsen, 1986; Tabor and Hudleston, 1991; Bauer et al., 1992).

The early folds are frequently nappe-like with thrusts (Poulsen et al., 1980; Borradaile, 1982; Davis et al., 1989; Percival, 1989; Tabor and Hudleston, 1991; Bauer et al., 1992), yielding overturned stratigraphy in many cases (Poulsen et al., 1980; Borradaile, 1982). Strike-slip faulting may have accompanied the nappe stacking and formed wrench-related basins (Poulsen, 2000; Czeck and Fralick, 2002). Despite its subvertical orientation, given the occurrence of few folds within its outcrop, the Seine Group is interpreted to be deposited during the wrench-related basin formation (Czeck and Fralick, 2002).

Evidence for the regional dextral shear includes: asymmetric pressure shadows adjacent to rigid clasts, foliation wrapping around rigid clasts indicating clast rotation, tiling of clasts, S–C structures, minor asymmetric Z folds, local sigmoid-shaped zones in which foliation varies in both orientation and intensity, foliation "fish" and shear bands, and back-rotated boudins (Poulsen, 2000; Czeck and Hudleston, 2003). These features commonly indicate subhorizontal, dextral shear roughly parallel with the subprovince boundaries (Poulsen, 2000; Czeck and Hudleston, 2003). Map-scale evidence of dextral shear is indicated by late-stage offsets along the major faults (Sims, 1976) and large sigmoidal outcrop patterns created by shear zones and foliation between major faults (e.g., Poulsen, 1986).

Previous strain analyses revealed a significant amount of flattening consistent with north–south tectonic shortening (Hsu, 1971; Kennedy, 1984; Tabor and Hudleston, 1991; Dehls, 1992; Czeck and Hudleston, 2003). The combination of the flattening strain, dextral shear-sense indicators, and subvertical foliations with mineral lineations obliquely plunging both eastward and westward (Fig. 4) is consistent with the interpretation of younger

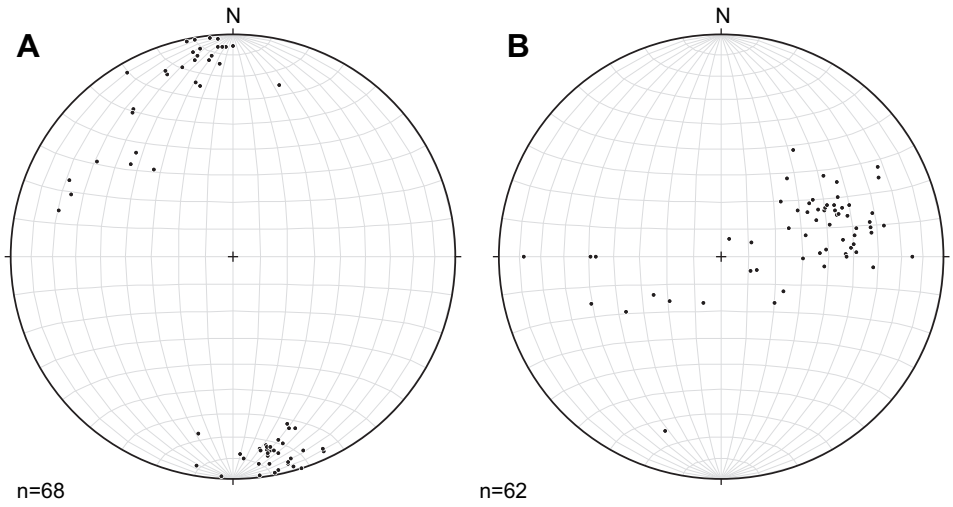

Fig. 4. Equal area stereonets of (A) poles to foliation and (B) lineation data from the Seine metaconglomerates. Both measurements are from preferred orientations of minerals in the matrix.

ductile transpressional deformation (Poulsen, 1986; Tabor and Hudleston, 1991; Borradaile and Dehls, 1993; Borradaile et al., 1993; Czeck and Hudleston, 2003) with a dominant pure shear component and variable non-vertical extrusion (Czeck and Hudleston, 2003, 2004).

3. Strain analysis

3.1. Methods

We conducted detailed strain analysis in the Seine metaconglomerates within the three-dimensional exposures along Ontario's Highway 11. First, we used large plastic sheets to trace clasts on relatively planar outcrop surfaces. Tracings of individual clasts were color-coded based on lithology. We measured a minimum of 50 each of felsic volcanic, mafic volcanic and granitoid clasts on each two-dimensional surface. Other clasts including gabbro, porphyritic volcanic rock, quartzite, and banded iron formation were traced but not analyzed due to their very small abundances. We measured conglomerate clasts on three to six planes (one or two sets of three roughly orthogonal planes) at each of the 26 outcrops analyzed.

We calculated two-dimensional finite strain for each lithological clast population on each tracing using the R_f/φ method (Ramsay, 1967; Dunnet, 1969; Lisle, 1985). The method assumes passive behavior of elliptical clasts and can be used to estimate the strength of preexisting sedimentary fabrics. The R_f/φ technique provides our best approximation of finite clast strain, although the assumption of passive behavior is incorrect in particular cases, as evidenced by foliation deflections around some clasts (Fig. 3C). Consequently, these results are minimum estimates of the true strain experienced by the clasts.

To test the internal consistency of our R_f/φ results, we applied the bootstrap statistical technique to the data. Bootstrap resampling consists of analyzing numerous subsets of true data with the R_f/φ method and averaging the results to decrease the impact of any potential clast that is a statistical outlier. The technique produces confidence ranges for the calculated average values of R_s and φ (McNaught, 2002; Mulchrone, 2005; Yonkee, 2005). In this study, 100 bootstrap data sets of 50 clasts each were created and analyzed from each field-measured clast data set (Table 1, Supplementary material).

The normalized Fry method at the outcrop scale should provide a best estimate of the bulk rock strain, whereas the normalized Fry method at a photomicrograph scale should provide a best estimate of the matrix strain (Treagus and Treagus, 2002). We attempted to use the normalized Fry method (Fry, 1979; Erslev and Ge, 1990; McNaught, 2002) to quantify bulk rock strain (Treagus and Treagus, 2002), but the results were clearly spurious. Most likely, the bulk rock strain estimates proved to be unreliable because clasts interacted during deformation and some clasts deformed in a brittle–ductile manner. Therefore, we do not consider our bulk rock strain results further.

After conducting two-dimensional strain analyses of the clasts, we used the resultant normalized aspect ratios and φ angle orientations to determine three-dimensional strain ellipsoids, assuming constant volume, by using the program "Ellipsoid 2003" (Launeau and Robin, 2003, 2005). This program allows the two-dimensional data to be weighted by the number of clasts when calculating the three-dimensional strain ellipsoid and produces error estimates for the best-fit ellipsoids. Most of our analyses (74 out of 78) were robust, but four analyses (stations C and P felsic clasts and stations P and Z mafic clasts) had large errors indicating very poor fits between the strain data and the calculated best-fit ellipsoid. Therefore, these four analyses were not used for effective viscosity estimates discussed later. Where we had six outcrop planes (21 out of 26 analyses), all were used to determine a single three-dimensional ellipsoid (Table 2, Supplementary material).

We use distinct parameters to describe the magnitude and shape of three-dimensional finite strain. Strain magnitude is quantified with octahedral shear strain, $\bar{\varepsilon}_s$, where $\bar{\varepsilon}_s = 0$ describes a sphere, and $\bar{\varepsilon}_s$ values increase as ellipsoid shapes grow more distorted (Nadai, 1963; Hsu, 1966; Hossack, 1968; Owens, 1984; Brandon, 1995). This parameter is useful because it allows comparison of strain magnitude from deformations with different strain paths. Lode's parameter, ν, describes strain shape and ranges from -1.0 to $+1.0$ where $\nu < 0$ for constrictional-type strains and $\nu > 0$ for flattening-type strains (Hossack, 1968). Strain magnitude, $\bar{\varepsilon}_s$, and the shape parameter, ν, were calculated from (Hossack, 1968):

$$\bar{\varepsilon}_s = \frac{\left[(\ln X - \ln Y)^2 + (\ln Y - \ln Z)^2 + (\ln Z - \ln X)^2\right]^{1/2}}{\sqrt{3}} \quad (1)$$

and

$$\nu = \frac{2(\ln Y - \ln X - \ln Z)}{\ln X - \ln Z}, \quad (2)$$

where *X*, *Y*, and *Z* are the normalized magnitudes of the maximum, intermediate, and minimum principal strain axes.

3.2. Results

Orientations of calculated strain axes (Fig. 5) are generally consistent at an individual outcrop regardless of clast type. The majority of long and intermediate axes of the strain ellipsoids for the clast populations trend approximately 070 to 100°, or 250 to 280° with varying plunges. Short axes trend approximately at 320 to 360° or 160 to 180° with shallow plunges. In most cases, the calculated long axes match the mineral lineation and short axes are normal to the foliation. Thus, primary clast fabrics have not significantly affected our results. This result corroborates our assumption that the calculated orientations of the principal axes determined through strain analysis truly represent the orientations of finite strain.

Strain magnitudes vary nonsystematically through the field region (Figs. 6 and 7A). Felsic metavolcanic clasts have $\overline{\varepsilon}_s$ values of 0.64 to 1.78 with a mean value of 1.30. Mafic metavolcanic clasts have $\overline{\varepsilon}_s$ values of 0.67 to 2.40 with a mean value of 1.29. For granitoid clasts, $\overline{\varepsilon}_s$ = 0.21 to 1.04 with a mean value of 0.51. In general, the mafic and felsic clast populations have similar strain magnitudes at a particular outcrop and granitoid clasts have consistently smaller strain magnitudes (Fig. 8). The regional-scale variations in strain magnitude cannot be linked to changes in the concentrations of clast types within the outcrops (Fissler, 2006). Instead, these variations may be related to spatial proximity to the minor shear zones.

Of the 26 outcrops evaluated, 19 have an overall flattening strain, five exhibited a constrictional strain, and two exhibited plane-strain (Figs. 6 and 7B). Flattening dominates throughout the field area while constriction exists in the western and easternmost stations (Fig. 7B). For felsic metavolcanic clasts, ν values range from −0.70 to 0.81, with a mean value of 0.34. The mafic metavolcanic clasts have ν values ranging from −0.40 to 0.80, with a mean value of 0.35. The granitoid clasts have ν values ranging from −0.43 to 0.89, with a mean value of 0.33. In most cases, all three clast types have either exclusively oblate or prolate shapes. However, a few cases exist where one clast population exhibits prolate strain shape where the others exhibit oblate strain shape, or vice versa. Strain magnitude does not correlate to strain shape (Fig. 9).

3.3. Clast comparisons

The patterns of strain magnitudes show some consistent patterns. First, within each clast population, the greatest strains are in the east. Second, the mafic clasts were usually strained the most,

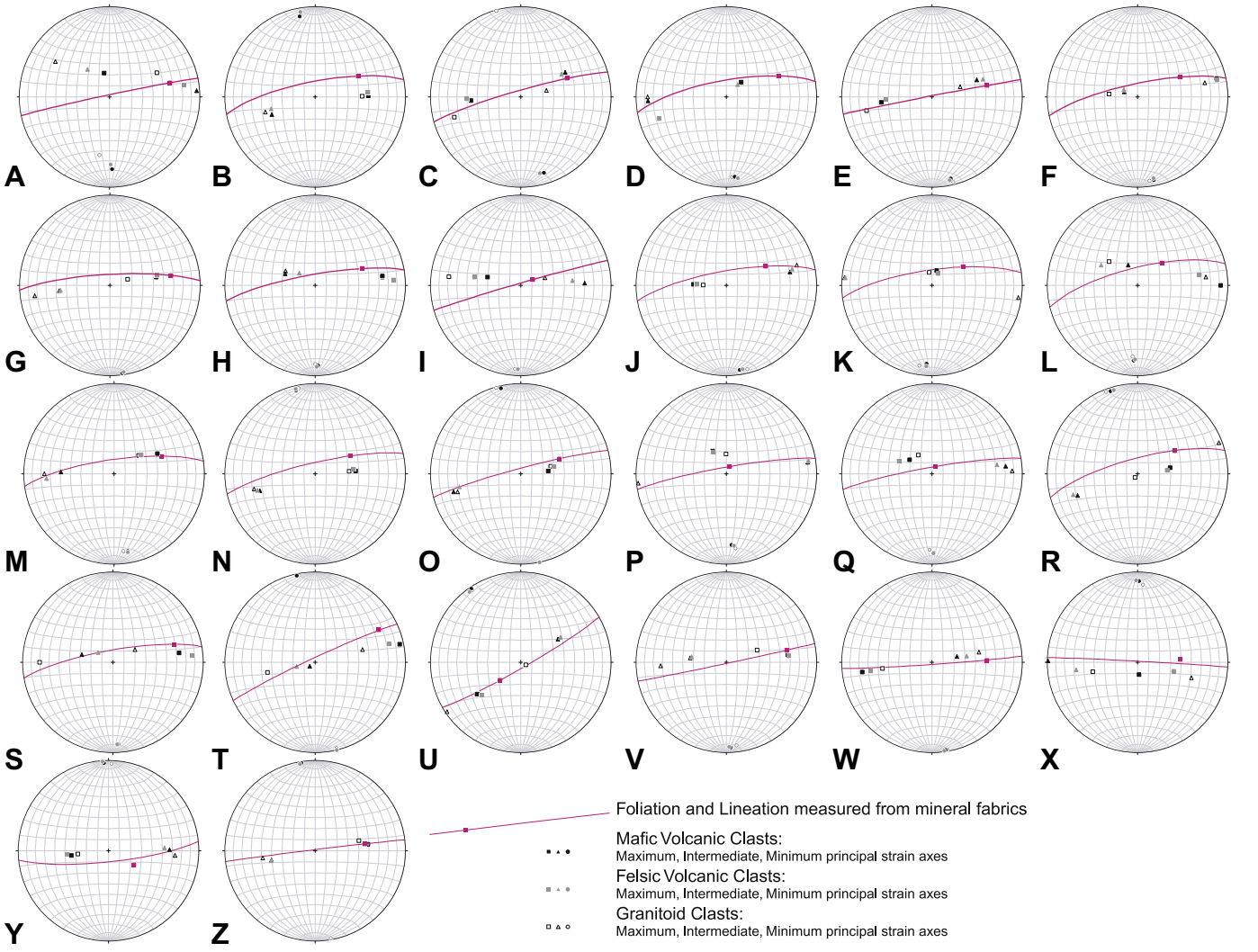

Fig. 5. Stereonets with orientations of *X*, *Y*, *Z* (maximum, intermediate, and minimum) principal strain orientations for outcrops A–Z. Foliations and lineations determined from mineral fabrics also shown for comparison.

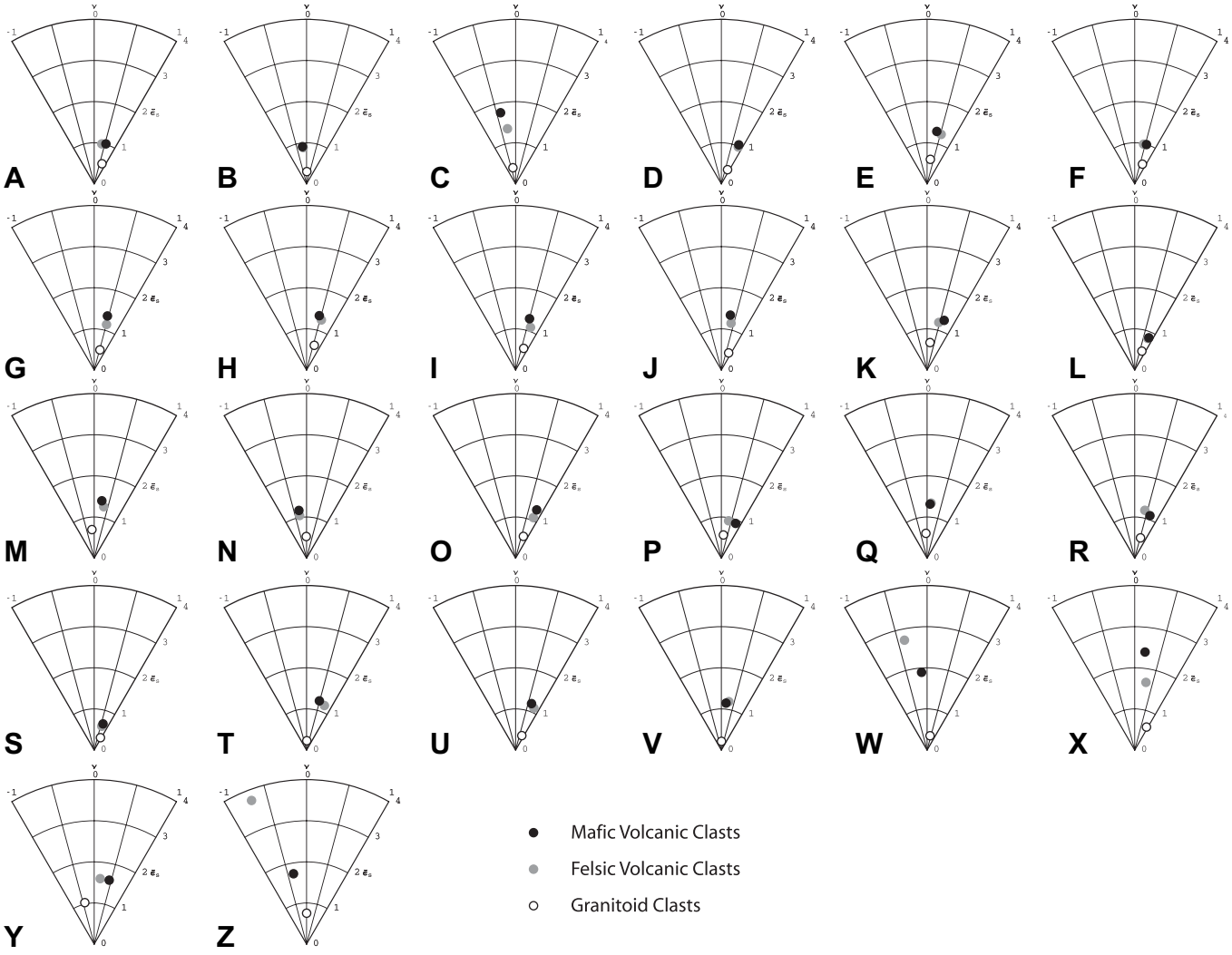

Fig. 6. Hsu plots indicating strain magnitudes ($\bar{\varepsilon}_s$) and strain shapes (ν) for outcrops A–Z.

and the granitoid clasts were strained the least (Figs. 6, 7A and 8). The felsic clasts strained most similarly to the mafic clasts (Figs. 6, 7A and 8). Third, in general, the three different clast populations showed the same approximate finite strain ellipsoid shape (i.e., oblate vs. prolate) at any particular outcrop.

Several features of the strain data were not anticipated. First, strain magnitude does not correlate to finite strain shape or geographic position (Figs. 7 and 9). Second, the different clast types show different finite strain ellipsoid shapes at some individual localities. For example, in six instances (outcrops B, M, Q, W, Y, and Z), some clast types are oblate and some are prolate. This effect is particularly true for the east end of the transect, which generally contains the greatest finite strain magnitudes. In these instances, there is not a consistent pattern of strain shape with clast type as one might expect from previous work that predicted more prolate shapes for more competent clasts (Freeman and Lisle, 1987).

4. Effective viscosity ratios

4.1. Methods used to calculate effective viscosity ratios

Effective viscosity describes the bulk flow behavior of a rock over a finite period of time (e.g., Treagus, 1999). The relative effective viscosities of different clast populations are evidenced by their different magnitudes of finite strain (Gay, 1968a,b; Lisle et al., 1983; Treagus and Treagus, 2002). Assuming Newtonian viscous rheological behavior, the effective viscosities of clasts can be related to their range of strain magnitudes.

We used the equation developed by Gay (1968a) for an elliptical inclusion in a matrix of contrasting viscosity to relate two-dimensional bulk strain, R_{bulk} (X/Z ratio), to clast strain, R_{clast} (X/Z ratio), assuming bulk pure shear and Newtonian clast viscosities for a given ratio of clast/bulk viscosity (V):

$$\ln R_{clast} = \ln R_{bulk}\left(\frac{5}{3+2V}\right). \quad (3)$$

This equation yields accurate results for geologically realistic bulk strains (Gay, 1976). The assumption of pure shear deformation ensures that our results are a minimum estimate of the true strain because pure shear distorts material more efficiently than simple shear or general shear such as transpression. While the conglomerates used in our study were not deformed via pure shear, they deformed via pure shear dominated transpression, so Eq. (3) is a reasonable approximation. The above equation holds true for all principal strain ratios (Treagus and Treagus, 2002); however, equations derived from multiple planes are not independent.

While this modeling is for two-dimensional circular objects embedded in a viscous matrix, Treagus and Treagus (2002)

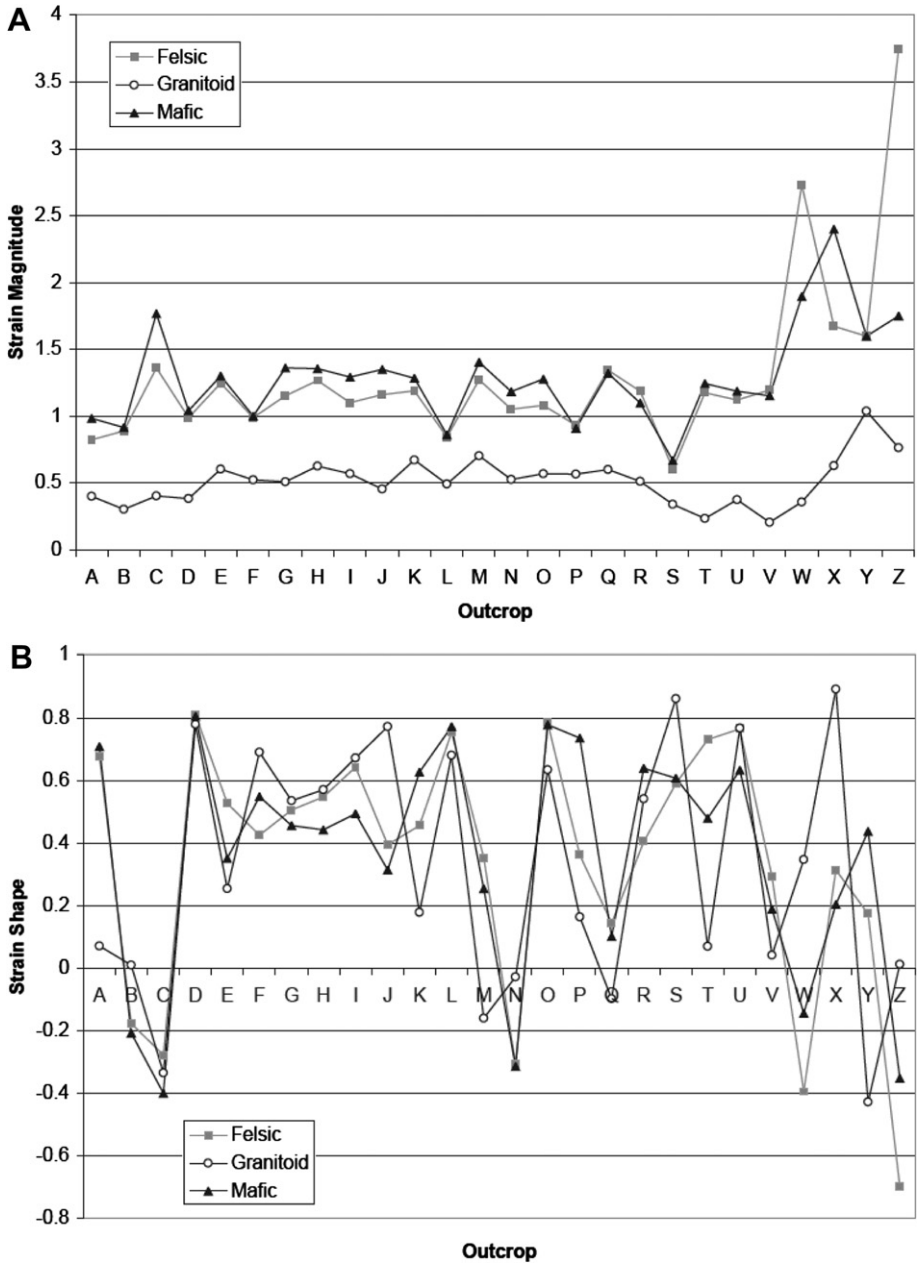

Fig. 7. Plots indicating (A) strain magnitudes ($\bar{\varepsilon}_s$) and (B) strain shapes (ν) from west to east across basin (stations A–Z).

assessed the inaccuracies of two-dimensional modeling for three-dimensional ellipsoidal clast shapes and determined that the errors were minimal ($\sim$5% in the *XZ* section). Thus, Eq. (3) yields favorable approximations for practical geological applications.

To best approximate bulk strain, we used the strain measured for the mafic volcanic clasts (Czeck and Hudleston, 2003). These clasts have very similar composition and mineralogy to the matrix and are typically the most volumetrically abundant clast type. The similarities in strain shapes and magnitudes between the second most abundant clast type, the felsic volcanics, lend support to this approximation. However, this approximation for bulk strain is likely a minimum estimate.

4.2. Analysis of effective viscosity ratios

The ratio between the effective viscosity of the felsic clasts and bulk effective viscosity (estimated from the mafic clasts) ranges from 0.27 to 2.12, with most values being close to 1 (Fig. 10A). These data suggest that the mafic and felsic clasts have very similar behaviors throughout the deformation. Effective viscosity ratios are commonly slightly greater than 1, indicating that felsic clasts are typically more viscous than mafic clasts or bulk rock.

The granitoid clasts have a very different behavior with respect to the bulk effective viscosity. The ratio between the granitoid clast effective viscosity and the bulk effective viscosity ranges from 2.35 to 12.39 (Fig. 10B). The effective viscosity ratios vary considerably, especially for smaller clast strains. While the relationship is not simple, the effective viscosity ratios generally decrease with increasing finite strain. In particular, stations with some of the most strongly deformed granitoid clasts (i.e., Stations K, M, Y) typically have smaller effective viscosity contrasts. Interestingly, some examples with relatively large bulk strains are not necessarily coincident with the stations with greatest granitoid clast strains (e.g., Station C).

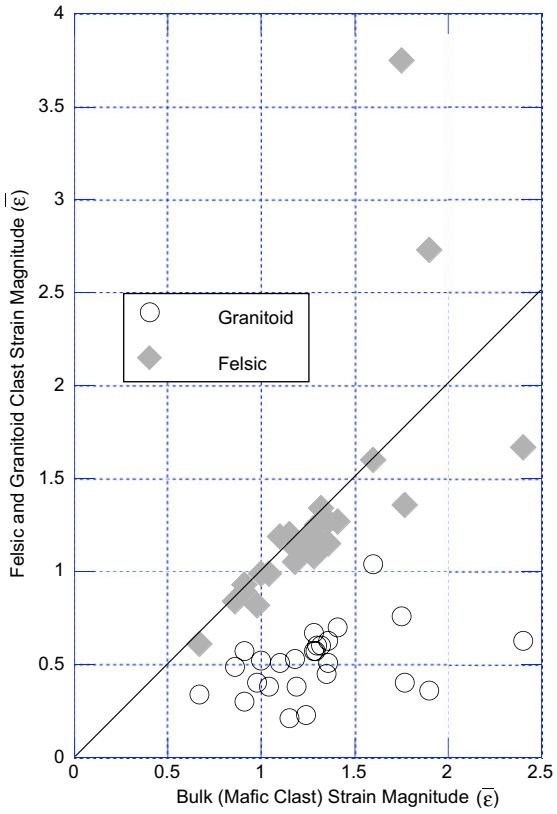

Fig. 8. Plot of granitoid and felsic clast strains vs. mafic clast strain (proxy for bulk strain). All strains plotted as strain magnitude ($\bar{\varepsilon}_s$). Line of equal strain magnitude is shown.

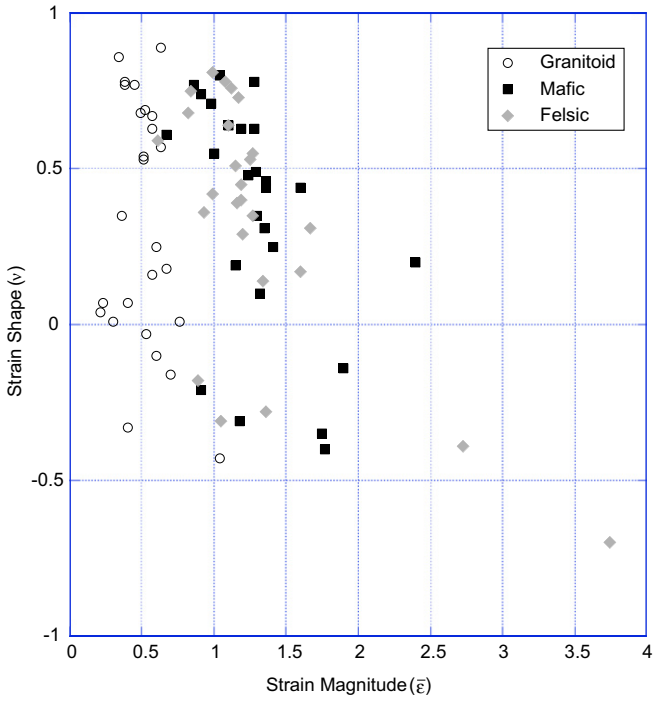

Fig. 9. Plot of strain shape (v) vs. strain magnitude (Es).

5. Discussion

A few key features stand out from these data. First, we note the hierarchy of competence with granitoid > felsic ≥ mafic. This hierarchy matches qualitative observations made from the field. These data can be used, in a qualitative way, to extract rheological information. For example, for granitoid clast strains (X/Z) of 2, the effective viscosity of granitoid clasts is approximately 3–6 times that of mafic and felsic clasts.

Factors that may control the relatively large effective viscosity of the granitoid clasts include: 1) lithology, and 2) grain size within a clast. Lisle and Savage (1982) noted that the most likely cause of rheological distinctions is grain size rather than rock composition. Our data support this idea in two ways. First, the overall composition of the felsic volcanic clasts is similar to the granitic clasts, yet they have very different grain sizes and effective viscosities. Second, the felsic volcanic clasts and the mafic volcanic clasts differ significantly in bulk composition, yet have similar grain sizes and effective viscosities.

The second major feature of the data is that the effective viscosity ratios, particularly of the granitoid clasts, do not remain constant throughout the field area or throughout the deformation. For small clast strains, granitoid ≫ felsic ≥ mafic. For large clast strains, granitoid > felsic ≥ mafic. This change in relative rheology may result from some combination of four factors: 1) the effective viscosity ratios are dependent on the magnitude of finite strain, 2) the effective viscosity ratios are dependent on clast ellipticity, 3) the effective viscosity ratios are dependent on deformation path, and/or 4) one or more of the clast types has a nonlinear rheology. In the following paragraphs, we consider each of these factors.

In the case of the Seine metaconglomerates, a strain gradient can be observed both qualitatively (Fig. 3) and quantitatively (Fig. 7A). In some cases, a demonstrable dependence also exists for the effective viscosity contrasts with clast strain (Fig. 10B), and clast strain is not linearly dependent on bulk strain. Therefore, the variable effective viscosity contrasts could be explained by a strain-dependent rheology such as those predicted by some modeling of multi-phase materials that simulate polymineralic rocks (Jordan, 1987; Takeda and Griera, 2006). In particular, the reduced effective viscosity ratio between granitoid and volcanic clasts with increasing strain could be explained if the granitoid clasts preferentially experienced some type of strain softening.

Measured clast ellipticity is a combination of original clast shape and the ellipticity induced by finite strain. Treagus and Treagus (2001) demonstrated that for circular or elliptical cylindrical objects imbedded in a matrix, strain is dependent on ellipticity in pure shear. For competent elliptical objects, the strain was greater than in circular objects of the same viscosity. For incompetent elliptical objects, the strain was smaller than in circular objects of the same viscosity. Relating these modeling results to geological situations, Treagus and Treagus (2001) postulated that these ellipticity effects should result in a decreased ductility contrast for competent clasts at larger strains, only be significant in geological situations when sectional elliptical ratios exceeded approximately 2, and be applicable to kinematic conditions other than pure shear.

In considering these findings within the context of the Seine metaconglomerates, the granitoid clasts behaved more competently than the matrix and other clasts, so one would expect that they would progressively strain more during each increment of deformation as their aspect ratios increased. Several of the measured outcrops (11 out of 26) have granitoid X/Z strain ratios >2 with the greatest X/Z ratio at Station Y ($X/Z = 3.35$). The X/Z ratio may be considered to be the greatest sectional axial ratio of the average clast, however individual clasts have greater axial ratios. The relative small degrees of ellipticity achieved by the competent granitoid clasts and the lack of a straight-forward relationship

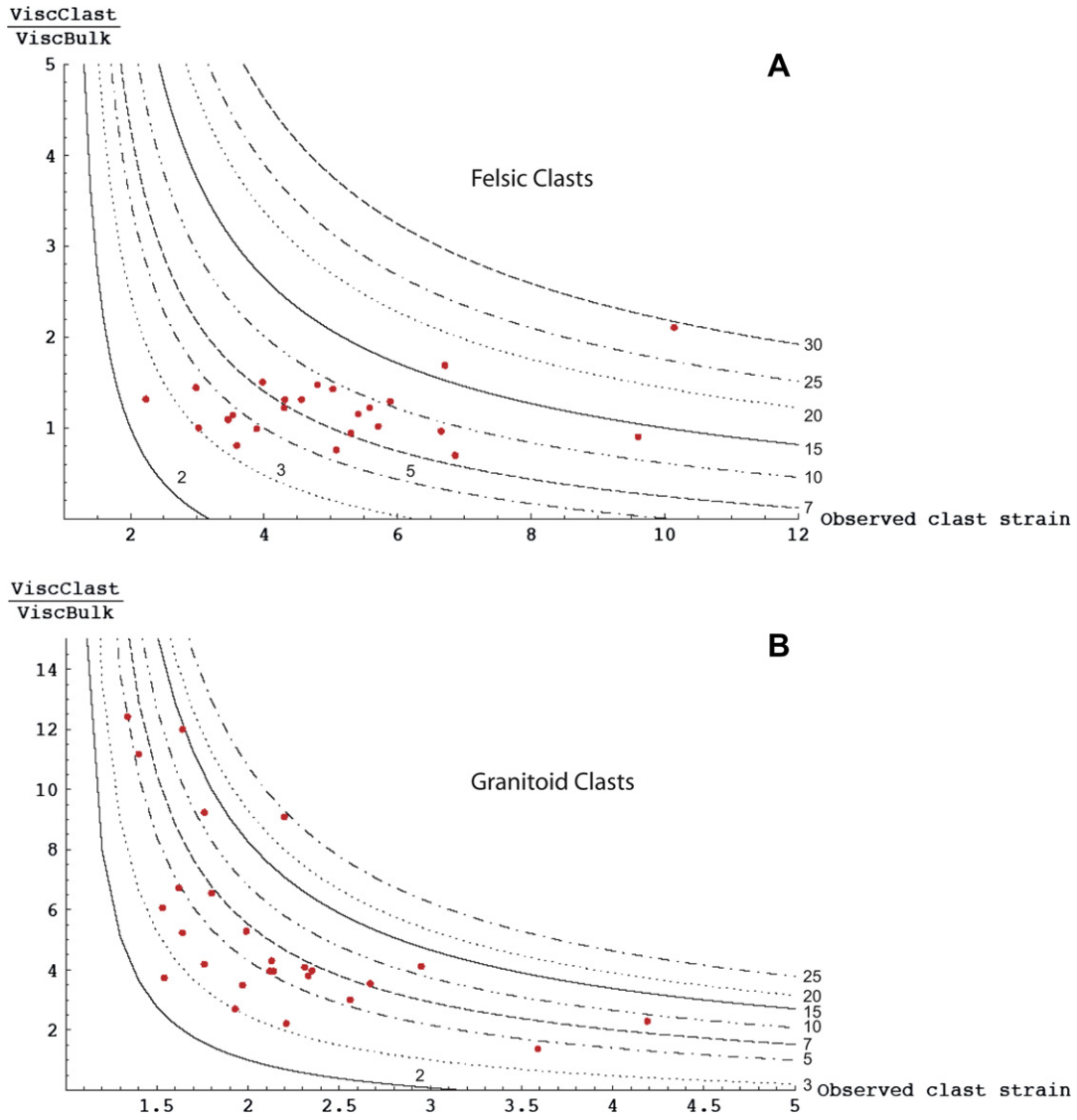

Fig. 10. Calculated effective viscosity ratios vs. clast strain ratios for (A) felsic clasts and (B) granitoid clasts indicating relative effective viscosity vs. strain. Strain given as X/Z ratios. Bulk effective viscosity is estimated as the effective viscosity of the mafic clasts. The effective viscosity ratios are not shown for those stations with significant errors of fit for three-dimensional strain. For felsic clasts, one outlier was omitted corresponding to Station W, where calculated X/Z value is 44 and calculated viscosity ratio is 0.27. Plotted curves are for bulk strain (X/Z) values as shown.

between the calculated effective viscosity ratios and granitoid clast ellipticity suggest that, in this case, the ellipticity effect may only partly explain the decreased ductility contrast between the granitoid clasts and matrix with increasing strain.

Considering the third factor, a demonstrable variability in deformation path must exist throughout the region because prolate and oblate finite strains do occur at some of the same stations, and finite strain shape does not relate to strain magnitude (Fig. 9). Deformation path variability could contribute to, but not entirely explain, the variable effective viscosity ratios because one would not expect a relationship between finite strain and effective viscosity contrast (Fig. 10) if the deformation path variability was solely responsible for the changes in effective viscosity contrast.

With respect to the fourth factor, the strain magnitudes (X/Z ratios) between our clast populations vary by less than an order of magnitude, suggesting that the range of effective viscosities is restricted to an order of magnitude or less. Many previous estimates also indicate that effective viscosities of rocks vary by less than a factor of ~10 (Gay, 1968a,b; Gay and Fripp, 1976; Huber-Aleffi, 1982; Lisle and Savage, 1982; Lisle et al., 1983; Roday et al., 1990; Kanagawa, 1993; Treagus and Treagus, 2002; Horsman et al., 2008), and this limited range supports the hypothesis that many rocks deform in an approximately Newtonian manner (Treagus, 1999; Treagus and Treagus, 2002).

However, some evidence suggests that at least some clasts did not deform in a linear viscous manner. From experimental work, we might expect power-law rheologies in certain minerals deformed by certain deformation processes (e.g., quartz in dislocation creep, Hirth and Tullis, 1992). Indeed, in all clast types within the Seine Group, microstructural evidence such as undulose extinction and subgrain formation in quartz and other minerals indicates dislocation creep was a likely prevalent deformation mechanism (Czeck, 2001; Fissler, 2006), and the rheology at this scale should thus be nonlinear. However, it remains an open question whether this would result in the larger-scale clast deforming in a manner that is significantly nonlinear. In fact, our results agree with many previous effective viscosity ratio estimates that indicate that effective viscosities of rocks vary by less than

a factor of ~10, in our case ~12 (Gay, 1968a,b; Gay and Fripp, 1976; Huber-Aleffi, 1982; Lisle and Savage, 1982; Lisle et al., 1983; Roday et al., 1990; Kanagawa, 1993; Treagus and Treagus, 2002; Horsman et al., 2008). This limited range of effective viscosity supports the hypothesis that many rocks deform with an approximately linear rheology over geological time scales (Treagus, 1999; Treagus and Treagus, 2002). The lack of pervasive necking or strain localization within our measured clasts also supports the linear rheology hypothesis. However, we do note that some clasts exhibit necking behavior, primarily when "wrapping" around more rigid clasts (Fig. 3C), which is only possible in nonlinear flow. As evidence for non-Newtonian rheology seems to be confined to some restricted cases, the variable effective viscosity ratios are likely to be primarily due to strain dependency rather than non-Newtonian rheology.

In summary, the variability of the relative effective viscosities between clasts is primarily due to strain-dependent rheologies. However, differences in deformation path may also contribute to the changing relative effective viscosities. Clast ellipticity and potential nonlinear rheologies produce minor contributions.

6. Conclusions

1. Distinct clast compositions (granitoid, felsic volcanic, mafic volcanic) in the Seine metaconglomerate record different amounts of finite strain for a given amount of bulk rock strain.
2. The competence hierarchy determined from three-dimensional strain analysis of granitoid > felsic ≥ mafic clasts agrees with inferences based on field observations of relative deformation behavior.
3. The finite strain data can be used to calculate effective viscosities assuming that the mafic clasts record the bulk strain, which is an appropriate assumption given that the mafic clasts are abundant and have similar composition to the matrix.
4. The greater effective viscosity of the granitic clasts is hypothesized to result from the relatively large grain size, relative to the volcanic clasts.
5. The effective viscosity ratios of the granitoid clasts do not remain constant across the strain gradient. For small strains, granitoid ≫ felsic ≥ mafic. For large strains, granitoid > felsic ≥ mafic. These data suggest that the effective viscosity ratios are dependent on the magnitude of finite strain and possibly also on deformation path.
6. The range of effective viscosity contrasts for different rock types, inferred from strain magnitudes, suggests that these rocks deformed in a Newtonian or nearly Newtonian manner. Non-Newtonian deformation would likely lead to an appreciably larger range of observed strain magnitudes.

Acknowledgements

We thank Peter Hudleston for introducing DC to the field area and Amanda Raitanen for assisting DF in the field. We thank Jordi Carreras and Sue Treagus for their suggestions, Richard Lisle and Mark McNaught for their reviews, and Associate Editor Bill Dunne for his revisions. This work was supported by National Science Foundation grant EAR-0510893 to DC and BT, a UWM Graduate School Research Committee Award to DC, a UWM RGI award to DC, and a Wisconsin Geological Society Scholarship (courtesy of the late Mrs. Ellen Brown) to DF.

Appendix. Supplementary data

Supplementary data associated with this article can be found, in the online version, at doi:10.1016/j.jsg.2009.08.004.

References

Bauer, R.L., Hudleston, P.J., Southwick, D.L., 1992. Deformation across the western Quetico subprovince and adjacent boundary regions in Minnesota. Canadian Journal of Earth Sciences 29, 2087–2103.
Borradaile, G.J., 1982. Comparison of Archean structural styles in two belts of the Canadian Superior Province. Precambrian Research 19, 179–189.
Borradaile, G.J., Dehls, J.F., 1993. Regional kinematics inferred from magnetic subfabrics in Archean rocks of northern Ontario, Canada. Journal of Structural Geology 15, 887–894.
Borradaile, G.J., Werner, T., Dehls, J.F., Spark, R.N., 1993. Archean regional transpression and paleomagnetism in northwestern Ontario, Canada. Tectonophysics 220, 117–125.
Brandon, M.T., 1995. Analysis of geologic strain data in strain-magnitude space. Journal of Structural Geology 17, 1375–1385.
Burke, K., Dewey, J.F., Kidd, W.S.F., 1976. Dominance of horizontal movements, arc and microcontinental collisions during the later permobile regime. In: Windley, B.F. (Ed.), The Early History of the Earth. John Wiley & Sons, New York, pp. 113–129.
Card, K.D., 1990. A review of the Superior Province of the Canadian Shield, a product of Archean accretion. Precambrian Research 48, 99–156.
Card, K.D., Ciesielski, A., 1986. DNAG subdivisions of the Superior Province of the Canadian Shield. Geoscience Canada 13, 5–13.
Czeck, D.M., 2001. Strain Analysis, Rheological Constraints, and Tectonic Model for an Archean Polymictic Conglomerate: Superior Province, Ontario, Canada. Ph. D. thesis. University of Minnesota.
Czeck, D.M., Fralick, P., 2002. Field trip 3: structure and sedimentology of the Seine conglomerate, Mine Centre area, Ontario. In: Proceedings and Abstracts – Institute on Lake Superior Geology 48, Part 1, pp. 37–67.
Czeck, D.M., Hudleston, P.J., 2003. Testing models for obliquely plunging lineations in transpression: a natural example and theoretical discussion. Journal of Structural Geology 25, 959–982.
Czeck, D.M., Hudleston, P.J., 2004. Physical experiment of vertical transpression with localized nonvertical extrusion. Journal of Structural Geology 26, 573–581.
Czeck, D.M., Maes, S.M., Sturm, C.L., Fein, E.M., 2006. Assessment of the relationship between emplacement of the Algoman plutons and regional deformation in the Rainy Lake region, Ontario. Canadian Journal of Earth Sciences 43, 1653–1671.
Davis, D.W., Poulsen, K.H., Kamo, S.L., 1989. New insights into Archean crustal development from geochronology in the Rainy Lake area, Superior Province, Canada. Journal of Geology 97, 379–398.
Dehls, J.F., 1992. The Magnetic Fabrics and Strain History of the Archean Seine Group Metasedimentary Rocks near Mine Centre, Northwestern Ontario. M.S. thesis. Lakehead University.
Druguet, E., Czeck, D.M., Carreras, J., Castaño, L.M., 2008. Emplacement and deformation features of syntectonic leucocratic veins from Rainy Lake zone (Western Superior Province, Canada). Precambrian Research 163, 384–400.
Dunnet, D., 1969. A technique of finite strain analysis using elliptical particles. Tectonophysics 7, 117–136.
Erslev, E.A., Ge, H., 1990. Least-squares center-to-center and mean object ellipse fabric analysis. Journal of Structural Geology 12, 1047–1059.
Fissler, D.A., 2006. A Quantitative Analysis of Strain in the Seine River Metaconglomerates, Rainy Lake region, Northwestern Ontario, Canada. M.S. thesis. University of Wisconsin-Milwaukee.
Fralick, P., Davis, D., 1999. The Seine-Coutchiching problem revisited: sedimentology, geochronology and geochemistry of sedimentary units in the Rainy Lake and Sioux Lookout Areas. In: Harrap, R.M., Helmstaedt, H. (Eds.), 1999 Western Superior Transect Fifth Annual Workshop 70. Lithoprobe Secretariat, University of British Columbia, pp. 66–75.
Frantes, J.R., 1987. Petrology and Sedimentation of the Archean Seine Group Conglomerate and Sandstone, Western Wabigoon Belt, Northern Minnesota and Western Ontario. M.S. thesis. University of Minnesota.
Freeman, B., Lisle, R.J., 1987. The relationship between tectonic strain and the three-dimensional shape fabrics of pebbles in deformed conglomerates. Journal of the Geological Society of London 144, 635–639.
Fry, N., 1979. Random point distributions and strain measurements in rocks. Tectonophysics 60, 89–105.
Gay, N.C., 1968a. Pure shear and simple shear deformation of inhomogeneous viscous fluids. 1. Theory. Tectonophysics 5, 211–234.
Gay, N.C., 1968b. Pure shear and simple shear deformation of inhomogeneous viscous fluids. 2. The determination of the total finite strain in a rock from objects such as deformed pebbles. Tectonophysics 5, 295–302.
Gay, N.C., 1976. The change of shape of a viscous ellipsoidal region embedded in a slowly deforming matrix having a different viscosity – a discussion. Tectonophysics 35, 403–407.
Gay, N.C., Fripp, R.E.P., 1976. The control of ductility on the deformation of pebbles and conglomerates. Philosophical Transactions of the Royal Society of London, Series A: Mathematical and Physical Sciences 238, 109–128.
Hirth, G., Tullis, J., 1992. Dislocation creep regimes in quartz aggregates. Journal of Structural Geology 14, 145–159.
Hoffman, P.F., 1989. Precambrian geology and tectonic history of North America. In: Bally, A.W., Palmer, A.R. (Eds.), The Geology of North America: an Overview. The Geology of North America A. Geological Society of America, Boulder, CO, pp. 447–512.

Hoffman, P.F., 1990. On accretion of granite–greenstone terrane. In: Robert, F., Sheahan, P.A., Green, S.B. (Eds.), Greenstone Gold and Crustal Evolution NUNA Conference Volume. Geological Association of Canada, St. John's, NF, pp. 32–45.

Horsman, E., Tikoff, B., Czeck, D.M., 2008. Rheological implications of heterogeneous deformation at multiple scales in the Late Cretaceous Sierra Nevada, California. Geological Society of America Bulletin 120, 238–255.

Hossack, J.R., 1968. Pebble deformation and thrusting in the Bygdin area (S. Norway). Tectonophysics 5, 315–339.

Hsu, M.-Y., 1971. Analysis of Strain, Shape, and Orientation of the Deformed Pebbles in the Seine River Area, Ontario. Doctoral thesis. McMaster University.

Hsu, T.C., 1966. The characteristics of coaxial and non-coaxial strain paths. Journal of Strain Analysis 1, 216–222.

Huber-Aleffi, A., 1982. Strain determinations in the conglomeratic gneiss of the Lebendun Nappe, Ticino, Switzerland. Geologica Romana 21, 235–277.

Hudleston, P.J., Holst, T.B., 1984. Strain analysis and fold shape in a limestone layer and implications for layer rheology. Tectonophysics 106, 321–347.

Hudleston, P.J., Lan, L., 1993. Information from fold shapes. Journal of Structural Geology 15, 253–264.

Hudleston, P.J., Lan, L., 1995. Rheological information from geological structures. Pure and Applied Geophysics 145, 605–620.

Jordan, P., 1987. The deformational behaviour of bimineralic limestone–halite aggregates. Tectonophysics 135, 185–197.

Kanagawa, K., 1993. Competence contrasts in ductile deformation as illustrated from naturally deformed chert-mudstone layers. Journal of Structural Geology 15, 865–885.

Kennedy, M.C., 1984. The Quetico Fault in the Superior Province of the southern Canadian Shield. M.S. thesis. Lakehead University.

Kirby, S.H., 1985. Rock mechanics observations pertinent to the rheology of the continental lithosphere and the localization of strain along shear zones. Tectonophysics 119, 1–27.

Kirby, S.H., Kronenberg, A., 1987. Rheology of the lithosphere: selected topics. Reviews of Geophysics 25, 1219–1244.

Kohlstedt, D.L., Evans, B., Mackwell, S.J., 1995. Strength of the lithosphere; constraints imposed by laboratory experiments. Journal of Geophysical Research 100, 17587–17602.

Langford, F.F., Morin, J.A., 1976. The development of the Superior Province of northwestern Ontario by merging island arcs. American Journal of Science 276, 1023–1034.

Launeau, P., Robin, P.-Y.F., 2003. Ellipsoid 2003. http://www.sciences.univ-nantes.fr/geol/UMR6112/SPO.

Launeau, P., Robin, P.-Y.F., 2005. Determination of fabric and strain ellipsoids from measured sectional ellipses – implementation and applications. Journal of Structural Geology 27, 2223–2233.

Lisle, R.J., 1985. Geological Strain Analysis: a Manual for the Rf/φ Method. Pergamon Press, Oxford.

Lisle, R.J., Rondeel, H.E., Doorn, D., Brugge, J., Van de Gaag, P., 1983. Estimation of viscosity contrast and finite strain from deformed elliptical inclusions. Journal of Structural Geology 5, 603–610.

Lisle, R.J., Savage, J., 1982. Factors influencing rock competence: data from a Swedish deformed conglomerate. Geologiska föreningens i Stockholm förhandlingar 104, 219–224.

Marquis, R., 2004. Towards a better understanding of the Superior Province. Quebec Mines. In: Mining Information Bulletin. http://www.mrnf.gouv.qc.ca/english/mines/quebec-mines/2004-10/superior.asp.

Masuda, T., Shibutani, T., Yamaguchi, H., 1995. Comparative rheological behaviour of albite and quartz in siliceous schists revealed by the microboudinage of piedmontite. Journal of Structural Geology 17, 1523–1533.

McNaught, M.A., 2002. Estimating uncertainty in normalized Fry plots using a bootstrap approach. Journal of Structural Geology 24, 311–322.

Mulchrone, K.F., 2005. An analytical error for the mean radial length method of strain analysis. Journal of Structural Geology 27, 1658–1665.

Nadai, A., 1963. Theory of Flow and Fracture of Solids, second ed. McGraw-Hill, New York.

Owens, W.H., 1984. The calculation of a best-fit ellipsoid from elliptical sections on arbitrarily orientated planes. Journal of Structural Geology 6, 571–578.

Paterson, M.S., 2001. Relating experimental and geological rheology. International Journal of Earth Sciences 90, 157–167.

Paterson, M.S., Luan, F.C., 1990. Quartzite rheology under geological conditions. In: Knipe, R.J., Rutter, E.H. (Eds.), Deformation Mechanisms, Rheology and Tectonics. Geological Society, London, Special Publications, vol. 54, pp. 299–307.

Percival, J.A., 1989. A regional perspective of the Quetico metasedimentary belt, Superior Province, Canada. Canadian Journal of Earth Sciences 26, 677–693.

Percival, J.A., Williams, H.R., 1989. Late Archean Quetico accretionary complex, Superior province, Canada. Geology 17, 23–25.

Poulsen, K.H., 1986. Rainy Lake wrench zone: an example of an Archean subprovince boundary in Northwestern Ontario. In: de Wit, M.J., Ashwal, L.D. (Eds.), Tectonic Evolution of Greenstone Belts Technical Report 86-10. Lunar and Planetary Institute, Houston, TX, pp. 177–179.

Poulsen, K.H., 2000. Archean Metallogeny of the Mine Centre – Fort Frances area. Ontario Geological Survey Report 266.

Poulsen, K.H., Borradaile, G.J., Kehlenbeck, M.M., 1980. An inverted Archean succession at Rainy Lake, Ontario. Canadian Journal of Earth Sciences 17, 1358–1369.

Ramsay, J.G., 1967. Folding and Fracturing of Rocks. McGraw-Hill, New York.

Ramsay, J.G., 1982. Rock ductility and its influence on the development of tectonic structures in mountain belts. In: Hsue, K.J. (Ed.), Mountain Building Processes. Academic Press, London, pp. 111–127.

Roday, P.P., Maheshwari, G., Vaghmarey, N.H., 1990. R_i-μ_i/μ_m-C_i dependent oblateness of deformed pebbles in the Baraitha conglomerate, central India and tectonic implications. Proceedings of the Indian Academy of Sciences: Earth and Planetary Sciences 99, 321–338.

Sims, P.K., 1976. Early Precambrian tectonic–igneous evolution in the Vermilion district, northeastern Minnesota. Geological Society of America Bulletin 87, 379–389.

Smith, R.B., 1975. Unified theory of the onset of folding, boudinage and mullion structure. Geological Society of America Bulletin 86, 1601–1609.

Smith, R.B., 1977. Formation of folds, boudinage and mullions in non-Newtonian materials. Geological Society of America Bulletin 88, 312–320.

Stone, D., Hallé, J., Murphy, R., 1997a. Precambrian Geology, Mine Centre Area. Ontario Geological Survey Preliminary Map P. 3372, Scale 1:50,000.

Stone, D., Hallé, J., Murphy, R., 1997b. Precambrian Geology, Mine Centre Area. Ontario Geological Survey Preliminary Map P. 3373, Scale 1:50,000.

Tabor, J.R., Hudleston, P.J., 1991. Deformation at an Archean subprovince boundary, northern Minnesota. Canadian Journal of Earth Sciences 28, 292–307.

Takeda, Y.-T., Griera, A., 2006. Rheological and kinematical responses to flow of two-phase rocks. Tectonophysics 427, 95–113.

Talbot, C.J., 1999. Can field data constrain rock viscosities? Journal of Structural Geology 21, 949–957.

Treagus, S.H., 1983. A theory of finite strain variation through contrasting layers, and its bearing on cleavage refraction. Journal of Structural Geology 5, 351–368.

Treagus, S.H., 1999. Are viscosity ratios measurable from cleavage refraction? Journal of Structural Geology 21, 895–901.

Treagus, S.H., Treagus, J.E., 2001. Effects of object ellipticity on strain, and implications for clast-matrix rocks. Journal of Structural Geology 23, 601–608.

Treagus, S.H., Treagus, J.E., 2002. Studies of strain and rheology of conglomerates. Journal of Structural Geology 24, 1541–1567.

Wood, J., Dekker, J., Jansen, J.G., Keay, J.P., Panagapko, D., 1980a. Mine Centre Area (Eastern Half), District of Rainy River. Ontario Geological Survey Preliminary Map P. 2202, Scale 1:15840.

Wood, J., Dekker, J., Jansen, J.G., Keay, J.P., Panagapko, D., 1980b. Mine Centre Area (Western Half), District of Rainy River. Ontario Geological Survey Preliminary Map P. 2201, Scale 1:15840.

Yonkee, A., 2005. Strain patterns within part of the Willard thrust sheet, Idaho–Utah–Wyoming thrust belt. Journal of Structural Geology 27, 1315–1343.